Available online at www.sciencedirect.com
SCIENCE DIRECT®
Journal of Solid State Chemistry 179 (2006) 413–420
JOURNAL OF SOLID STATE CHEMISTRY
www.elsevier.com/locate/jssc

Metal phosphonates based on aminomethylenediphosphonate: Syntheses and characterization of $Na_4Zn\{NH_3CH(PO_3)_2\}_2 \cdot 4H_2O$, $Ni\{NH_3CH(PO_3H)_2\}_2 \cdot xH_2O$ and $NaNi_2\{NH_3CH(PO_3)(PO_3H_{0.5})\}_2(H_2O)_2 \cdot 2H_2O$

Song-Song Bao, Tian-Wei Wang, Yi-Zhi Li, Li-Min Zheng*

State Key Laboratory of Coordination Chemistry, Coordination Chemistry Institute, Nanjing University, Nanjing 210093, PR China

Received 9 August 2005; received in revised form 25 October 2005; accepted 26 October 2005
Available online 1 December 2005

Abstract

This paper describes the syntheses of three transition metal diphosphonate compounds: $Na_4Zn\{NH_3CH(PO_3)_2\}_2 \cdot 4H_2O$ (**1**), $Ni\{NH_3CH(PO_3H)_2\}_2 \cdot xH_2O$ (**2**) and $NaNi_2\{NH_3CH(PO_3)(PO_3H_{0.5})\}_2(H_2O)_2 \cdot 2H_2O$ (**3**). Compound **1** contains chains of $[Zn\{NH_3CH(PO_3)_2\}_2]_n^{4n-}$ made up of corner-sharing ZnO_6 octahedra and CPO_3 tetrahedra, which are further connected by tetramers of edge-sharing NaO_6 octahedra, forming a three-dimensional open-framework structure. Compound **2** shows a square-grid layer structure where the NiO_6 octahedra are corner shared with CPO_3 tetrahedra. The adjacent layers are linked by strong interlayer hydrogen bonds, resulting in a three-dimensional open-network structure with channels where the lattice water molecules reside. The structure of compound **3** is analogous to that of $NaCo_2\{NH_3CH(PO_3)(PO_3H_{0.5})\}_2(H_2O)_2 \cdot xH_2O$ in which layers of $Ni_2\{NH_3CH(PO_3)(PO_3H_{0.5})\}_2(H_2O)_2$ are connected by NaO_6 linkages into an open-framework structure. The magnetic studies show that weak antiferromagnetic interactions are mediated between the nickel ions in compounds **2** and **3**. Crystal data for **1**: triclinic, space group $P\bar{1}$, $a = 5.551(2)$ Å, $b = 6.166(2)$ Å, $c = 12.424(4)$ Å, $\alpha = 92.422(6)^\circ$, $\beta = 92.687(7)^\circ$, $\gamma = 93.926(6)^\circ$, $V = 423.3(2)$ Å^3, $Z = 2$. For **2**: triclinic, space group $P\bar{1}$, $a = 9.043(1)$ Å, $b = 9.180(1)$ Å, $c = 9.271(1)$ Å, $\alpha = 89.693(3)^\circ$, $\beta = 70.202(3)^\circ$, $\gamma = 89.530(3)^\circ$, $V = 724.1(2)$ Å^3, $Z = 2$.

Keywords: Zinc; Nickel; Phosphonate; Aminomethylenediphosphonate; Crystal structure; Antiferromagnetic exchange

1. Introduction

The phosphonate chemistry has been of increasing interest due to their potential applications in ion exchange, catalysts, protonic conductors and sensors [1]. Among the various metal phosphonate compounds reported so far, those with open-framework or porous structures have received particular attentions [2]. Such compounds maybe obtained by using methylenediphosphonate and its derivatives $[O_3PC(R)(R')PO_3]$ [3]. In a previous communication, we reported a cobalt compound $NaCo_2\{NH_3CH(PO_3)(PO_3H_{0.5})\}_2(H_2O)_2 \cdot xH_2O$ [4] based on aminomethylenediphosphonate [*amdp*, $NH_2CH(PO_3)_2$] which shows an interesting open-framework structure. In this paper, three new metal–*amdp* compounds with three-dimensional open-framework or network structures are described, namely $Na_4Zn\{NH_3CH(PO_3)_2\}_2 \cdot 4H_2O$ (**1**), $Ni\{NH_3CH(PO_3H)_2\}_2 \cdot xH_2O$ (**2**) and $NaNi_2\{NH_3CH(PO_3)(PO_3H_{0.5})\}_2(H_2O)_2 \cdot 2H_2O$ (**3**). To the best of our knowledge, compounds **1**–**3** are the only metal–*amdp* compounds that have been structurally characterized except $NaCo_2\{NH_3CH(PO_3)(PO_3H_{0.5})\}_2(H_2O)_2 \cdot xH_2O$, although the bonding properties of this ligand with metal ions such as Fe^{3+}, In^{3+}, Gd^{3+}, Nd^{3+} and UO_2^{2+} have been studied in solution [5].

*Corresponding author. Fax: +86 25 83314502.
E-mail address: lmzheng@nju.edu.cn (L.M. Zheng).

0022-4596/$ - see front matter © 2005 Elsevier Inc. All rights reserved.
doi:10.1016/j.jssc.2005.10.041

2. Experimental

2.1. Materials and methods

Aminomethylenediphosphonic acid [$NH_2CH(PO_3H_2)_2$, *amdp*H_4] was prepared according to the literature [6]. All the other starting materials were of reagent-grade quality and were obtained from commercial sources without further purification. The elemental analyses were performed in a PE240C elemental analyzer. The infrared spectra were recorded on a VECTOR 22 spectrometer with pressed KBr pellets. Thermal analyses were performed in nitrogen in the temperature range 30–800 °C with a heating rate of 5 °C/min on a TGA-DTA V1.1b Inst 2100 instrument. The powder XRD patterns were recorded on a Shimadzu XD-3A X-ray diffractometer. The magnetic susceptibility data were obtained on polycrystalline samples (7.08 mg for **2** and 12.41 mg for **3**) using a Quantum Design MPMS-XL7 SQUID magnetometer. Diamagnetic corrections were estimated from Pascal's constants [7].

2.2. Synthesis of *1*

A mixture of $Zn(en)_2Cl_2$ (0.0513 g, 0.2 mmol), *amdp*H_4 (0.1142 g, 0.6 mmol), 1 M NaOH (3 cm^3) and H_2O(5 cm^3), adjusted by 1 M HCl to pH = 9.5 was hydrothermally treated at 140 °C for 2 d. After slow cooling to room temperature, square block-like colorless crystals of **1** were collected as a monophasic material, judged by the powder X-ray diffraction pattern. Yield: 75% based on Zn. Found (calcd.) for $C_2H_{16}N_2ZnNa_4O_{16}P_4$: C, 2.80 (3.96); H, 2.58 (2.64); N, 4.64 (4.62)%. IR (KBr, cm^{-1}): 3415–2620b, 1694w, 1644m, 1603m, 1539s, 1349w, 1147s, 1117s, 1069s, 1040s, 988s, 945s, 806m, 735m, 620m, 557s, 457s. Thermal analysis reveals that compound **1** starts to decompose on heating from room temperature. The weigh loss between 50 and 130 °C is 11.8%, corresponding to the removal of four water molecules (11.9%).

2.3. Synthesis of *2*

Hydrothermal treatment of a mixture of $NiSO_4 \cdot 6H_2O$ (0.0526 g, 0.2 mmol), *amdp*H_4 (0.1142 g, 0.6 mmol), 1 M NaOH (3 cm^3) and H_2O (5 cm^3), adjusted by 1 M HCl to pH = 1.5 at 140 °C for 3 d results in square sheet-like primrose yellow crystals of **2** as a monophasic material, judged by the powder X-ray diffraction pattern. Yield: 60% based on Ni. Found (calcd.) for $Ni\{NH_3CH(PO_3H)_2\}_2 \cdot 1.7H_2O$: C, 3.35 (5.11); H, 3.55 (3.28); N, 5.68 (5.97)%. IR (KBr, cm^{-1}): 3531sh, 3404w, 3110–2630b, 1636m, 1541m, 1316w, 1120s, 1000s, 931m, 888m, 810m, 726w, 556m, 419m. Thermal analysis reveals that the weigh loss between 50 and 130 °C is 6.2%, in agreement with the removal of 1.7 lattice water molecules (calcd. 6.5%).

2.4. Synthesis of *3*

Hydrothermal treatment of a mixture of $NiSO_4 \cdot 6H_2O$ (0.0526 g, 0.2 mmol), *amdp*H_4 (0.1142 g, 0.6 mmol), 1 M NaOH (3 cm^3) and H_2O (5 cm^3), adjusted by 1 M HCl to pH = 2.2, at 140 °C for 3 d results in needle-like yellow crystals of **3** with a yield of 80% based on Ni. Found (calcd.) for $C_2H_{17}O_{16}N_2P_4Ni_2Na$: C, 4.07 (2.59); H, 2.88 (2.87); N, 4.75 (4.90)%. IR (KBr, cm^{-1}): 3450–2910b, 1640m, 1520m, 1116s, 991m, 936m, 796m, 564m, 461w, 430w. Thermal analysis of **3** shows several steps of decomposition in the temperature range 50–600 °C. The weigh loss between 50 and 220 °C is 6.2%, corresponding to the removal of two lattice water molecules (calcd. 6.1%). The weight loss between 240 and 440 °C is 5.3%, close to the release of two coordinated water molecules (calcd. 6.1%).

2.5. Crystallographic studies

The data collections for complexes **1** and **2** were carried out on a Bruker SMART APEX CCD diffractometer equipped with graphite-monochromatized Mo$K\alpha$ ($\lambda = 0.71073$ Å) radiation at 298 K. A hemisphere of data was collected in the θ range 1.6–26.0° for **1** and 2.2–25.5° for **2** using a narrow-frame method with scan widths of 0.30° in ω and an exposure time of 10 s/frame. Numbers of the observed and unique reflections are 2263 and 1612 ($R_{int} = 0.0224$) for **1** and 3758 and 2626 ($R_{int} = 0.0254$) for **2**, respectively. The data were integrated using the Siemens SAINT program [8], with the intensities corrected for Lorentz factor, polarization, air absorption, and absorption due to variation in the path length through the detector faceplate. Empirical absorption and extinction corrections were applied.

The structures were solved by direct method and refined on F^2 by full-matrix least squares using SHELXTL [9]. All the non-hydrogen atoms in compounds **1** and **2** were refined anisotropically. All the hydrogen atoms were put on calculated positions or located from the Fourier maps and refined isotropically with the isotropic vibration parameters related to the non-H atom to which they are bonded. Crystallographic and refinement details are listed in Table 1. The selected bond lengths and angles for compounds **1** and **2** are given in Tables 2 and 3, respectively. CCDC-286617 (**1**) and 286616 (**2**) contain the supplementary crystallographic data for this paper.

3. Results and discussion

3.1. Syntheses

Compounds **1**–**3** have been prepared by reactions of metal sources and *amdp*H_4 (molar ratio 1:3) under hydrothermal conditions. It is found that the pH value plays a critical role in producing pure phases of **1**–**3**. Compound **1** resulted when the pH of the reactant mixture

Table 1
Crystallographic data for **1** and **2**

Formula	$C_2H_{16}N_2ZnNa_4O_{16}P_4$(1)	$C_2H_{18}NiN_2O_{15}P_4$(2)
M	605.40	492.77
Crystal size	$0.2 \times 0.2 \times 0.05$	$0.25 \times 0.25 \times 0.1$
Crystal system	Triclinic	Triclinic
Space group	P-1	P-1
a (Å)	5.551(2)	9.043(1)
b (Å)	6.166(2)	9.180(1)
c (Å)	12.424(4)	9.271(1)
α (deg)	92.422(6)	89.693(3)
β (deg)	92.687(7)	70.202(3)
γ (deg)	93.926(6)	89.530(3)
Z	2	2
V (Å^3)	423.3(2)	724.1(2)
D_c (g cm^3)	2.375	2.260
F(000)	304	504
Goodness-of-fit on F^2	0.990	1.161
$R1$, w$R2$[a] [$I > 2\sigma(I)$]	0.0556, 0.1289	0.0561, 0.1211
(All data)	0.0759, 0.1357	0.0725, 0.1253
$(\Delta\rho)_{max}$, $(\Delta\rho)_{min}$ (e/Å^3)	0.50, −0.88	0.47, −0.74

[a] $R_1 = \Sigma \| F_o \| - \| F_c \| / \Sigma \| F_o \|$. R_ = [(F_ - F_)^ /(F_)^]^1/2.

Table 2
Selected bond lengths (Å) and angles (deg) for **1**

Zn(1)–O(1)	2.107(4)	P(1)–O(1)	1.542(4)
Zn(1)–O(4)	2.085(4)	P(1)–O(2)	1.503(5)
Zn(1)–O(6B)	2.189(4)	P(1)–O(3)	1.532(4)
O(4)–Zn(1)–O(1)	89.58(16)	O(1)–Zn(1)–O(6B)	91.21(16)
O(4A)–Zn(1)–O(1)	90.42(16)	O(4)–Zn(1)–O(6C)	90.86(16)
O(4)–Zn(1)–O(6B)	89.14(16)	O(1)–Zn(1)–O(6C)	88.79(16)
P(1)–O(1)–Zn(1)	126.1(2)	Zn(1)–O(4)–Na(1)	96.67(17)
Zn(1)–O(1)–Na(1G)	136.1(2)	P(2)–O(6)–Zn(1F)	151.8(3)
P(2)–O(4)–Zn(1)	130.3(2)	Zn(1F)–O(6)–Na(1F)	92.62(16)

Symmetry transformations used to generate equivalent atoms: A: $-x+1, -y+1, -z+1$; B: $-x, -y+1, -z+1$; C: $x+1, y, z$; D: $x, y-1, z$; E: $-x, -y, -z$; F: $x-1, y, z$; G: $x, y+1, z$.

Table 3
Selected bond lengths (Å) and angles (deg) for **2**

Ni(1)–O(1)	2.062(4)	Ni(2)–O(2B)	2.054(4)
Ni(1)–O(5)	2.032(4)	Ni(2)–O(10)	2.054(4)
Ni(1)–O(7)	2.063(4)	Ni(2)–O(9)	2.082(4)
P(1)–O(1)	1.509(4)	P(3)–O(7)	1.481(4)
P(1)–O(2)	1.506(4)	P(3)–O(8)	1.584(4)
P(1)–O(3)	1.567(4)	P(3)–O(9)	1.508(4)
P(2)–O(4)	1.498(4)	P(4)–O(10)	1.498(4)
P(2)–O(5)	1.498(4)	P(4)–O(11)	1.509(4)
P(2)–O(6)	1.536(4)	P(4)–O(12)	1.531(4)
O(5)–Ni(1)–O(1)	90.60(15)	O(2B)–Ni(2)–O(10)	87.92(15)
O(5)–Ni(1)–O(1A)	89.40(15)	O(2C)–Ni(2)–O(10)	92.08(15)
O(5)–Ni(1)–O(7)	88.72(15)	O(2B)–Ni(2)–O(9)	88.41(15)
O(5A)–Ni(1)–O(7)	91.28(15)	O(2C)–Ni(2)–O(9)	91.59(15)
O(1)–Ni(1)–O(7)	89.43(16)	O(10)–Ni(2)–O(9)	93.11(15)
O(1)–Ni(1)–O(7A)	90.57(16)	O(10D)–Ni(2)–O(9)	86.89(15)
P(1)–O(1)–Ni(1)	131.7(2)	P(1)–O(2)–Ni(2E)	142.6(2)
P(2)–O(5)–Ni(1)	125.9(2)	P(3)–O(9)–Ni(2)	131.1(2)
P(3)–O(7)–Ni(1)	142.0(3)	P(4)–O(10)–Ni(2)	123.1(2)

Symmetry transformations used to generate equivalent atoms: A: $-x+1, -y, -z+2$; B: $x, y+1, z$; C: $-x+1, -y, -z+1$; D: $-x+1, -y+1, -z+1$; E: $x, y-1, z$.

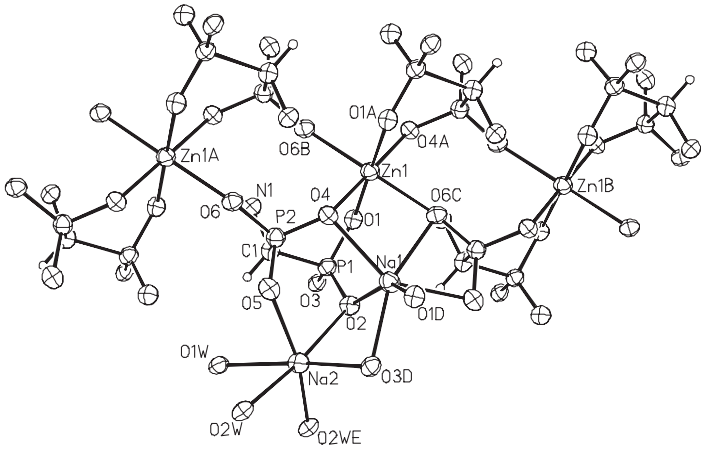

Fig. 1. Building unit of structure **1** with the atomic labeling scheme (thermal ellipsoids shown at 50% probability).

was high (9.0–9.5). At lower pH (2.0–8.0), clear solution is observed. A pure phase of compound **2** can be obtained only when the pH value is adjusted to ca. 1.5. When the pH is a little higher (2.2–2.5), a pure phase of compound **3** resulted. If the pH value were between 1.7 and 1.9, a mixture of compounds **2** and **3** would be produced. Reactions at a lower (<1.4) or higher (>3.0) pH values result in a mixture of unrecognized yellow and white precipitates. Hydrothermal reactions with other metal:*amdp*H_4 ratios (1:0.5, 1:1 and 1:2) were also performed under same conditions, yielding compounds **1**–**3** as powder or polycrystalline materials.

3.2. Description of the structures

Compound **1** crystallizes in triclinic space group *P*-1. The asymmetric unit consists of a half Zn atom, two Na atoms, one *amdp*H^{3-} ligand and two water molecules. As shown in Fig. 1, the coordination geometry around the zinc atom is distorted octahedral, defined by six phosphonate oxygen atoms [O(1), O(4), O(1*A*), O(4*A*), O(6*B*), O(6*C*)] from four equivalent *amdp*H^{3-} ligands. The Zn–O bond distances fall in the range 2.085(4)–2.189(4) Å. Each *amdp*H^{3-} acts as a zwitterionic tridentate ligand with the amino group protonated. It chelates to the same Zn atom through phosphonate oxygens O(1) and O(4), and bridges to the adjacent Zn atom through phosphonate oxygen O(6). Thus an infinite chain of $[Zn\{NH_3CH(PO_3)_2\}]_n^{4n-}$ is formed running along the *a*-axis which contains corner-sharing ZnO_6 octahedra and CPO_3 tetrahedra (Fig. 1). Similar chains have been found in compounds $(H_3NCH_2CH_2NH_3)M(hedpH_2)_2\cdot 2H_2O$ [M = Ni, Zn; *hedp* = $CH_3C(OH)(PO_3)_2$] [10] and $NaZn\{Cl_2C(PO_3)(PO_3H)\}\cdot 5H_2O$ [11]. The remaining three phosphonate oxygen atoms [O(2), O(3) and O(5)] are coordinated to the Na atoms.

Both Na(1) and Na(2) atoms locate at general positions and have distorted octahedral geometries. The Na(2)O_6 octahedron is edge-shared with both its equivalent through O(2w) and Na(1)O_6 octahedron through phosphonate oxygens O(2) and O(3), leading to a tetramer. The Na–O distances are between 2.246(5) and 2.631(5) Å. Subsequently, neighboring chains of $[Zn\{NH_3CH(PO_3)_2\}]_n^{4n-}$ are connected through tetramers of edge-sharing NaO_6 octahedra, forming a three-dimensional open-framework structure (Fig. 2). Extensive hydrogen bonds are observed among the water molecules, amino groups and phosphonate oxygen atoms. The three shortest contacts are 2.656(6), 2.724(7) and 2.789(6) Å for $N(1)\cdots O(5^{i})$, $N(1)\cdots O(1^{ii})$ and $O(1W)\cdots O(2^{ii})$, respectively (symmetry codes: i: x, $y+1$, z; ii: $x-1$, y, z).

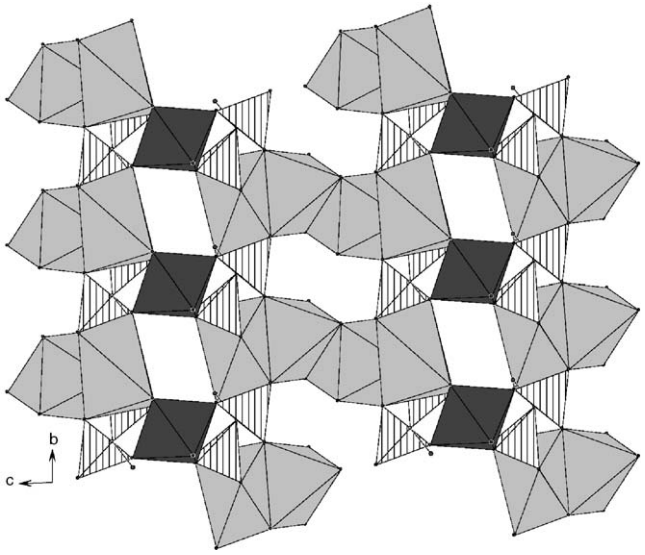

Fig. 2. Structure **1** packed along the [100] direction. All the H atoms are omitted for clarity. The ZnO_6 and NaO_6 octahedra and CPO_3 tetrahedra are presented as dark gray, medium gray and shaded polyhedra, respectively.

Compound **2** crystallizes in triclinic space group *P*-1. The asymmetric unit of the structure contains two Ni atoms (each with 50% occupancies), two *amdp*H_2^{2-} ligands and three water molecules. Both Ni(1) and Ni(2) atoms locate at inversion centers while the rest at general positions. Fig. 3 shows the coordination geometries around the Ni atoms. Each Ni atom has a distorted octahedral

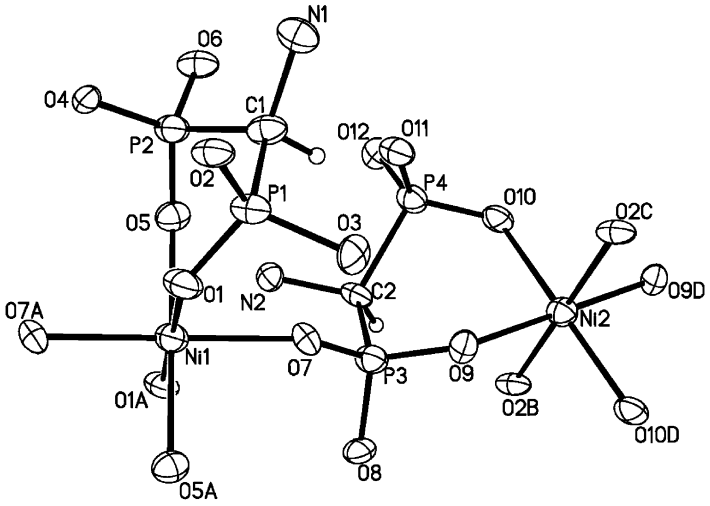

Fig. 3. Building unit of structure **2** with the atomic labeling scheme (thermal ellipsoids shown at 50% probability).

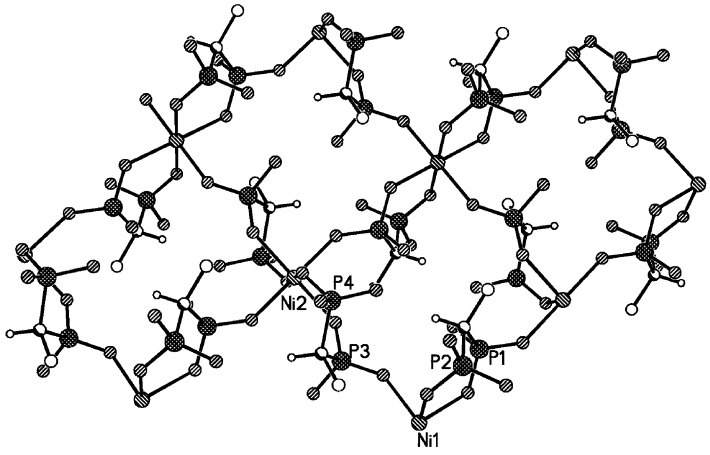

Fig. 4. One layer of structure **2** viewed along *a*-axis.

environment. All of its six binding sites are provided by phosphonate oxygens from two pairs of $amdpH_2^{2-}$ groups. The Ni–O bond lengths fall in the range of 2.032(5)–2.082(4) Å, in agreement with those in the other nickel phosphonate compounds such as $[H_3N(CH_2)_2NH_3]Ni(hedpH_2)_2\cdot 2H_2O$, $[H_3N(CH_2)_3NH_3]Ni(hedpH_2)_2(H_2O)$, $[H_3N(CH_2)_4NH_3]Ni(hedpH_2)_2(H_2O)_2$ [10a], $(NH_4)_2Ni(hedpH_2)_2(H_2O)_2\cdot 7H_2O$ [12], $[(CH_2CH_2OH)_3NH]Ni(hedpH_2)_2(H_2O)_2\cdot 5H_2O$ [13], $Ni_4\{CH_2(PO_3)_2\}_2$ [3c], $Ni_4\{CH_2(PO_3)_2\}_2(H_2O)_2$ [3c], and $Ni_4\{CH_2(PO_3)_2\}_2(H_2O)_3$ [3c]. Two types of aminomethylenediphosphonate ligands are found in the structure. Each behaves as a zwitterionic tridentate ligand, and chelates and bridges the Ni(1) and Ni(2) atoms through phosphonate oxygens O(1), O(2), O(5) and O(7), O(9), O(10), respectively. A square-grid layer of $[Ni\{NH_3CH(PO_3H)_2\}_2]_n$ is thus constructed in the *bc* plane (Fig. 4). The remaining three phosphonate oxygens of each $amdpH_2^{2-}$ ligand are either protonated [P(1)–O(3): 1.567(5) Å; P(2)–O(6): 1.536(4) Å; P(3)–O(8): 1.583(4) Å; P(4)–O(12): 1.532(4) Å] or pendant [P(2)–O(4): 1.498(4) Å; P(4)–O(11): 1.508(4) Å]. The adjacent layers are fused together through strong inter-layer hydrogen bonds, resulting in a supramolecular network structure with channels generated along the *b*-axis (Fig. 5). The shortest contacts between the layers are 2.561(5) and 2.442(5) Å for $O(6)\cdots O(11^{i})$ and $O(12)\cdots O(12^{ii})$ (symmetry codes: i, $2-x$, $-y$, $1-z$; ii, $2-x$, $1-y$, $1-z$), respectively. The lattice water molecules reside in the channels.

Compound **3** is isostructural to $NaCo_2\{NH_3CH(PO_3)(PO_3H_{0.5})\}_2(H_2O)_2\cdot xH_2O$ [4], based on their powder XRD patterns (Fig. 6). The unit cell refinement of compound **3**, by the aid of program TREOR90, reveals that the compound crystallizes in monoclinic lattice with parameters $a = 18.246(9)$ Å, $b = 9.648(8)$ Å, $c = 10.082(5)$ Å, $\beta = 104.72(4)^\circ$, $V = 1716.5$ Å^3. These parameters are close to those of $NaCo_2\{NH_3CH(PO_3)(PO_3H_{0.5})\}_2(H_2O)_2\cdot xH_2O$ [$a = 18.772(4)$ Å, $b = 9.417(2)$ Å, $c = 9.612(2)$ Å, $\beta = 102.593(4)^\circ$, $V = 1658.4(6)$ Å^3] [4]. Therefore, structure **3** can be described as an open-framework structure made up of $Ni_2\{NH_3CH(PO_3)(PO_3H_{0.5})\}_2(H_2O)_2$ layers containing four- and eight-member rings with NaO_6 linkages.

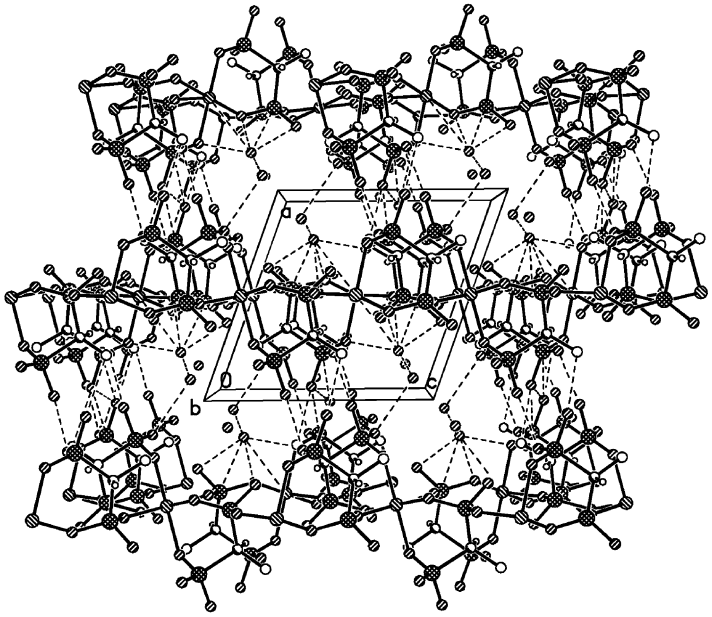

Fig. 5. Structure **2** packed along the [010] direction. All the H atoms are omitted for clarity.

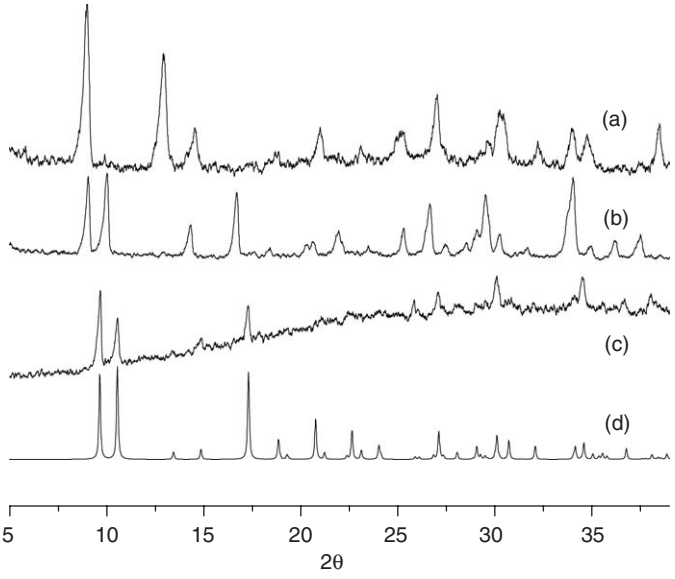

Fig. 6. Powder X-ray diffraction patterns for compounds **2** (a), **3** (b) and $NaCo_2\{NH_3CH(PO_3)(PO_3H_{0.5})\}_2(H_2O)_2 \cdot xH_2O$ ((c) experimental; (d) simulated from single crystal data).

It is of interest to compare structures of **1**–**3** with those of the corresponding metal–*hedp* compounds. Both *amdp*H_4 and *hedp*H_4 acids contain two phosphonate groups separated by one methyl group. Therefore, both can chelate the metal ions by using two or four of their six phosphonate oxygen atoms forming stable six-member rings of *M*–O–P–C–P–O, and bridge the neighboring metal ions by the rest phosphonate oxygen atoms (Scheme 1). In the case of metal–*hedp* system, the hydroxyl group of $hedp^{4-}$ is frequently found to serve as a donor in coordination with metal ions. Hence a series of compounds with formulas $[H_3N(CH_2)_nNH_3]M_2(hedpH)_2 \cdot 2H_2O$, $(NH_4)_2M_2(hedpH)_2$ and $[H_3N(C_6H_4)NH_3]M_2(hedpH)_2 \cdot H_2O$ (M = Zn, Co, Fe, Mn) [10b,14] have been reported showing double chain structures. In the case of metal–*amdp* system, however, the amino group of $amdp^{4-}$ is protonated and is involved only in the hydrogen bond network. It is thus not unexpected that the metal–*amdp* complexes would exhibit different structures from those of the metal–*hedp* compounds.

Although the chain structure of compound **1** is analogous to that in $(H_3NCH_2CH_2NH_3)M(hedpH_2)_2 \cdot 2H_2O$ (M = Ni, Zn), the structures of compounds **2** and **3** are unique. Compound **2** has a square-grid layer structure containing eight-member rings where $\{NiO_6\}$ octahedra are corner-shared with the $\{CPO_3\}$ tetrahedra. Compound **3** is isostructural to $NaCo_2\{NH_3CH(PO_3)(PO_3H_{0.5})\}_2(H_2O)_2 \cdot xH_2O$, with an open-framework structure made up of $M_2\{NH_3CH(PO_3)(PO_3H_{0.5})\}_2(H_2O)_2$ layers containing four- and eight-member rings with NaO_6 linkages. Similar topologies have not been found in the Ni-*hedp* systems. For example, $[H_3N(CH_2)_4NH_3]Ni(hedpH_2)_2(H_2O)_2$ [10], $Ni(hedpH_2)_2(H_2O)_2 \cdot 7H_2O$ [12] and $[(CH_2CH_2OH)_3NH]Ni(hedpH_2)_2(H_2O)_2 \cdot 5H_2O$ [13] are mononuclear compounds. In $[H_3N(CH_2)_3NH_3]Ni(hedpH_2)_2(H_2O)$ and $[H_3N(CH_2)_2NH_3]Ni(hedpH_2)_2 \cdot 2H_2O$ [10a], dinuclear and chain structures are found. The structures of compounds **1**–**3** are also distinguished from those of Ni(Zn)-methylenediphosphonate compounds reported so far. In compound $Ni_4\{CH_2(PO_3)_2\}_2(H_2O)_3$ [3c], a layer structure is found where NiO_6 octahedra and diphosphonate groups are grafted on the sheets of trimeric edge-sharing units of NiO_6 octahedra. Compounds $Ni_4\{CH_2(PO_3)_2\}_2(H_2O)_2$ [3c] and $Ni_4\{CH_2(PO_3)_2\}_2$ [3c] have three-dimensional structures by sharing

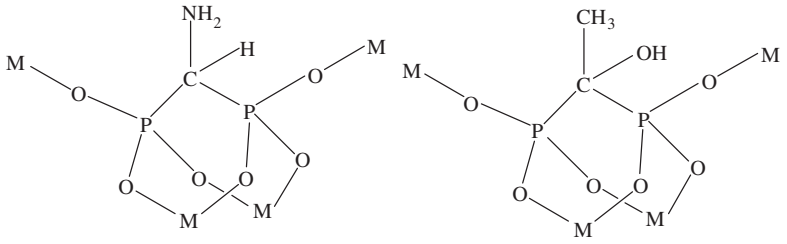

Scheme 1.

the fourth nickel cation between the layers of the $Ni_4\{CH_2(PO_3)_2\}_2(H_2O)_3$. Three-dimensional structures are also found in compounds $Zn_4\{CH_2(PO_3)_2\}_2(H_2O)_2$ [3d] and $Zn_4\{CH_2(PO_3)_2\}_2$ [3d].

3.3. Magnetic properties

Fig. 7 shows the temperature-dependent molar magnetic susceptibilities of compound **2** over the temperature range 2–300 K, measured at 2 kOe. The plots for compound **3** are provided as Supporting material. For **2**, the effective magnetic moment per Ni at 300 K is 2.89 μ_B, in agreement with the theoretical value (2.83 μ_B) for a single Ni(II) ion ($S = 1$, $g = 2.0$). For **3**, the effective magnetic moment per Ni_2 at 300 K is 4.66 μ_B, close to the theoretical value (4.00 μ_B) for two isolated Ni(II) ions ($S = 1$, $g = 2.0$). In both cases, the magnetic susceptibility data obey the Curie–Weiss law in the temperature range 50–300 K with Weiss constants −21.7 K for **2** and −34.0 K for **3**, respectively. The appearance of a maximum in the χ_M versus T plot and the decreasing of the $\chi_M T$ value upon cooling suggest dominant antiferromagnetic interactions between the Ni(II) centers in both cases.

Since compound **2** has a square-grid layer structure in which the Ni(II) ions are linked by O–P–O units, the magnetic susceptibility data of compound **2** were initially analyzed by the expression reported by Lines for a 2D square-planar Heisenberg model [15]. The attempt was, however, not successful. The intraplanar exchange constant J/k was thus derived by equation: $\tau = kT_{max}/|J|$ $S(S+1)$ [16], where the position of the maximum (T_{max}) in the χ_M versus T plot is related directly to the intraplanar exchange constant. For system with $S = 1$, $\tau = 2.20$. From the χ_M versus T plot of compound **2**, T_{max} is 19.65 K. Hence the estimated J/k value is −4.46 K. The magnetic properties of compound **3** can be treated in a similar way. In this case, the T_{max} is 14.88 K, and the estimated J/k value is −3.38 K. These J values are comparable to the other nickel phosphonate compounds with layered or pillared layered structures such as $Ni(RPO_3)(H_2O)$ ($J/k = -1.5$ K for $R = CH_3$, C_2H_5; −2.5 K for $R =$ phenyl), $Ni(CH_3PO_3)(H_2O)$ ($J/k = -2.7$ K) and $Ni_2(O_3PC_6H_4PO_3)(H_2O)_2$ ($J/k = -2.3$ K) [17]. It has to be noted that in the χ_M versus T plot of compound **3**, a small peak appears below 6 K. This could be due to the presence of a very small amount of impurities which cannot be identified by the XRD measurements. The possibility of long-range antiferromagnetic ordering also cannot be fully ruled out at this stage.

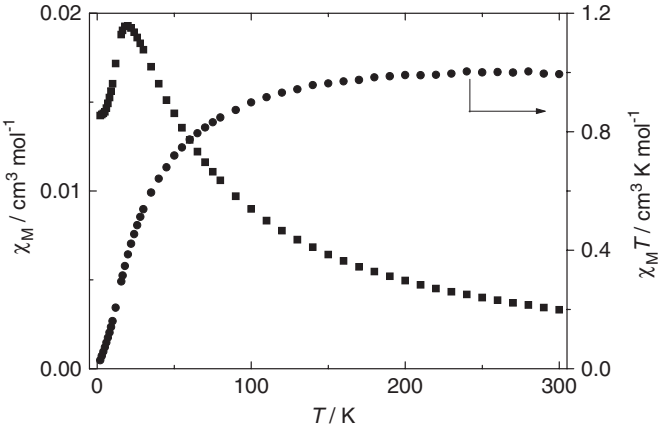

Fig. 7. The χ_M and $\chi_M T$ versus T plots for compound **2**.

4. Conclusions

This paper reports zinc and nickel diphosphonate compounds **1**–**3**. Compound **1** has a three-dimensional structure in which chains of $[Zn\{NH_3CH(PO_3)_2\}_2]_n$ are connected by tetramers of edge-sharing NaO_6 octahedra linkages. Compound **2** exhibits a square-grid layer structure, built up from the distorted NiO_6 octahedra and CPO_3 tetrahedra. Compound **3** shows an open-framework structure in which layers of $Ni_2\{NH_3CH(PO_3)(PO_3H_{0.5})\}_2(H_2O)_2$ are connected by NaO_6 linkages. Antiferromagnetic interactions are found in compounds **2** and **3**.

Acknowledgments

We thank the NNSF of China (No. 20325103), the Ministry of Education of China and the NSF of Jiangsu province (No. BK2002078) for financial supports and Mr. Y.-J. Liu for crystal data collection.

Appendix A. Supplementary materials

Supplementary data associated with this article can be found in the online version at doi:10.1016/j.jssc.2005.10.041.

References

[1] (a) A. Clearfield, Prog. Inorg. Chem. 47 (1998) 371;
(b) G. Cao, H. Hong, T.E. Mallouk, Acc. Chem. Res. 25 (1992) 420;
(c) G. Alberti, U. Constantino, M. Casciola, R. Vivani, Adv. Mater. 8 (1996) 291;
(d) V.V. Krishnan, A.G. Dokoutchaev, M.E. Thompson, J. Catal. 196 (2000) 366;
(e) C. Maillet, P. Janvier, M. Pipelier, T. Praveen, Y. Andres, B. Bujoli, Chem. Mater. 13 (2001) 2879.

[2] K. Maeda, Micropor. Mesopor. Mater. 73 (2004) 47.

[3] (a) D.L. Lohse, S.C. Sevov, Angew. Chem., Int. Ed. Engl. 36 (1997) 1619;
(b) D. Riou, O. Roubeau, G. Ferey, Micropor. Mesopor. Mater. 23 (1998) 23;
(c) Q.M. Gao, N. Guillou, M. Nogues, A.K. Cheetham, G. Ferey, Chem. Mater. 11 (1999) 2937;
(d) K. Barthelet, C. Merlier, C. Serre, M. Riou-Cavellec, D. Riou, G. Ferey, J. Mater. Chem. 12 (2002) 1132;
(e) P. Yin, L.-M. Zheng, S. Gao, X.-Q. Xin, Chem. Commun. (2001) 2346.

[4] S.-S. Bao, L.-M. Zheng, Y.-J. Liu, W. Xu, S.-H. Feng, Inorg. Chem. 42 (2003) 5037.

[5] (a) J.E. Bollinger, D.M. Roundhill, Inorg. Chem. 32 (1993) 2821;
(b) J.E. Bollinger, D.M. Roundhill, Inorg. Chem. 33 (1994) 6421.

[6] B. Bogdan, D. Marcin, J.B. Malgorzata, K. Tamas, H. Koslowski, J. Chem. Soc., Dalton Trans. (1997) 973.

[7] O. Kahn, Molecular Magnetism, VCH Publishers, Inc., New York, 1993.

[8] SAINT, Program for Data Extraction and Reduction, Siemens Analytical X-ray Instruments, Madison, WI, 1994–1996.

[9] SHELXTL (version 5.0) Reference Manual, Siemens Industrial Automation, Analytical Instrumentation, Madison, WI, 1995.

[10] (a) H.-H. Song, L.-M. Zheng, C.-H. Lin, S.-L. Wang, X.-Q. Xin, S. Gao, Chem. Mater. 11 (1999) 2382;
(b) H.-H. Song, L.-M. Zheng, Z. Wang, C.-H. Yan, X.-Q. Xin, Inorg. Chem. 40 (2001) 5024.

[11] M. Kontturi, E. Laurila, S. Peraniemi, J.J. Vepsalainen, M. Ahlgren, Inorg. Chem. 44 (2005) 2400.

[12] V.S. Sergienko, E.G. Afonin, G.G. Aleksandrov, Koord. Khim. 24 (1998) 293.

[13] V.S. Sergienko, G.G. Aleksandrov, E.G. Afonin, Kristallografiya 45 (2000) 262.

[14] (a) L.-M. Zheng, H.-H. Song, C.-H. Lin, S.-L. Wang, Z. Hu, Z. Yu, X.-Q. Xin, Inorg. Chem. 38 (1999) 4618;
(b) H.-H. Song, L.-M. Zheng, G. Zhu, Z. Shi, S. Feng, S. Gao, X.-Q. Xin, Chin. J. Inorg. Chem. 18 (2002) 67;
(c) H.-H. Song, P. Yin, L.-M. Zheng, J.D. Korp, A.J. Jacobson, S. Gao, X.-Q. Xin, J. Chem. Soc. Dalton Trans. (2002) 2752;
(d) L.-M. Zheng, S. Gao, P. Yin, X.-Q. Xin, Inorg. Chem. 43 (2004) 2151;
(e) P. Yin, L.-M. Zheng, X.-Q. Xin, Chem. Mater. 15 (2003) 3233;
(f) P. Yin, S. Gao, Z.-M. Wang, C.-H. Yan, L.-M. Zheng, X.-Q. Xin, Inorg. Chem. 44 (2005) 2761.

[15] M.E. Lines, J. Phys. Chem. Solids 31 (1970) 101.

[16] J. DeJongh, A.R. Miedema, Adv. Phys. 23 (1974) 1.

[17] (a) J. LeBideau, C. Payen, B. Bujoli, P. Palvadeau, J. Rouxel, J. Magn. Magn. Mater. 140–144 (1995) 1719;
(b) C. Bellitto, E.M. Bauer, S.A. Ibrahim, M.R. Mahmoud, G. Righini, Chem. Eur. J. 9 (2003) 1324;
(c) D.-K. Cao, S. Gao, L.-M. Zheng, J. Solid State Chem. 177 (2004) 2311.